Peculiarity in the Electronic Structure of Cu(II) Complex Ferromagnetically Coupled with Bisimino Nitroxides

Tadaaki Ikoma,*,†,‡ Hiroki Oshio,§ Masashi Yamamoto,⊥ Yasunori Ohba,¶ and Masayuki Nihei§

Institute of Science and Technology, Niigata University, 2-8050 Ikarashi, Nishiku, Niigata 950-2181, Japan, and PRESTO, Japan Science and Technology Agency, 4-1-8 Honcho, Kawaguchi 332-0012, Japan, and Graduate School of Pure and Applied Science, Department of Chemistry, University of Tsukuba, Tennodai 1-1-1, Tsukuba 305-8571, Japan, and Department of Chemistry, Graduate School of Science, Tohoku University, Sendai 980-8578, Japan, and Institute of Multidisciplinary Research for Advanced Materials, Tohoku University, Sendai 980-8577, Japan

Received: March 29, 2008; Revised Manuscript Received: June 9, 2008

By means of the electron spin resonance (ESR) technique, we have investigated the electronic structures of the tridentate imino nitroxyl diradical complex with copper(II) (Cu−bisimpy), which has a square planar structure and a ground quartet state with an extremely strong ferromagnetic exchange interaction, and its related compounds (bisimpy = 2,6-bis(1′-oxyl-4′,4′,5′,5′-tetramethyl-4′,5′-dihydro-1′*H*-imidazol-2′-yl)pyridine). It was clarified that Cu−bisimpy had unique magnetic orbitals, compared with the biradical ligand (bisimpy), a zinc(II) biradical complex (Zn−bisimpy) and a copper(II) terpyridine complex (Cu−tpy) (tpy = 2,2′;6′,2″-terpyridine). Multifrequency ESR spectroscopy provided a reliable set of magnetic parameters of Cu−bisimpy, which has a small *g* anisotropy ($g_x = 2.02$, $g_y = 2.01$, $g_z = 2.08$) and small hyperfine coupling with Cu ($|A_x| = 42.0$ MHz, $|A_y| \leq 14$ MHz, $|A_z| = 153$ MHz) but huge zero-field splitting ($D = +17.4$ GHz, $E = -1.0$ GHz). The maximum principal axis of zero-field interaction (z_{ZF}) is perpendicular to the *z* axis for the **g** and **A** tensors, which is normal to the molecular plane. These characteristics of the magnetic properties prove that the substantial spin transfer from the $d_{x^2-y^2}$ orbital of copper to the n-orbitals of the ligand is caused by a σ-type covalent bonding effect between the central metal and the ligand nitrogens. The covalent bonding effect produces carbene configurations on the nitrogen atoms of the imino nitroxyl radicals. The carbene configuration was concluded to be the main reason for the strong ferromagnetic coupling in Cu−bisimpy. Multifrequency electron spin resonance spectroscopy clarified the unique electronic structure of a square planar copper(II) complex with an imino nitroxyl diradical, which undergoes a strong ferromagnetic interaction caused by a covalent bonding effect.

Introduction

Among many strategies that have been developed for designing molecular magnets that are alternatives to conventional magnets, the metal-radical approach has led to promising results.[1–4] Especially, stable nitroxide radical complexes with copper(II, $3d^9$ configuration) ion as a building block have been well investigated for the last two decades.[5,6] In complexes where Cu^{2+} coordinates with the nitroxide oxygens, the axial coordination of the nitroxide group generally results in moderate ferromagnetic interactions, whereas the equatorial coordination tends to be antiferromagnetic.[7–13] The magnetic interaction is associated with the bonding character in the axial and equatorial coordination. When the nitroxide is axially coordinated to copper ion, the magnetic orbitals of π^* in nitroxide and $3d_{x^2-y^2}$ in Cu^{2+} are essentially orthogonal to each other and have a nonbonding relationship. In the equatorial coordination, a nonzero overlap between the magnetic orbitals occurs and leads to the bonding character. On the other hand, it has been discovered that Cu-complexes bonded with nitrogens of imino nitroxide radical ligands in equatorial coordination are ferromagnetic, of which the coupling constant (more than $+100$ cm^{-1}) is larger than that of Cu-complexes axially bonded with nitroxide oxygen.[14–18] So far, the size difference in the exchange coupling constant (*J*) is mainly discussed based on the bond length of the Cu−N equatorial coordination (typically 2.0 Å) which is shorter than that of the Cu−O axial coordination (2.3−2.4 Å). Recently, we also found a square planar complex of Cu^{2+} and bisimino nitroxides (Cu−bisimpy), forming the Cu−N equatorial coordination, as shown in Figure 1 that shows a ground quartet state ($S = 3/2$) because of a strong ferromagnetic coupling ($J = +165$ cm^{-1}).[19] The biradical ligand (2,6-bis(1′-oxyl-4′,4′,5′,5′-tetramethyl-4′,5′-dihydro-1′*H*-imidazol-2′-yl)pyridine; bisimpy), in which two imino nitroxides are linked at the ortho positions of pyridine, functions as a chelating reagent for metal chlorides in alcohol solvent and forms complexes with Cu^{2+} and zinc(II, $3d^{10}$ configuration). The magnetic interactions for bisimpy and the Zn^{2+} complex (Zn−bisimpy) are ferromagnetic, but the size of the exchange coupling constant (*J*) is much smaller than that of Cu−bisimpy. Unrestricted Hartree−Fock plus density functional hybrid calculations of d−p conjugated systems point out that the spin polarization and delocalization determine the sign of *J* in the transition metal and radical complexes.[20] It is therefore desired to determine the electronic structure of N-bonded Cu−bisimino nitroxide complexes to understand the

* To whom correspondence should be addressed. E-mail: ikoma@chem.sc.niigata-u.ac.jp. Telephone: +81-25-262-7390. Fax: +81-25-262-7390.
† Institute of Science and Technology, Niigata University.
‡ PRESTO, JST.
§ Department of Chemistry, University of Tsukuba.
⊥ Department of Chemistry, Tohoku University.
¶ IMRAM, Tohoku University.

10.1021/jp802810s CCC: $40.75
Published on Web 08/20/2008

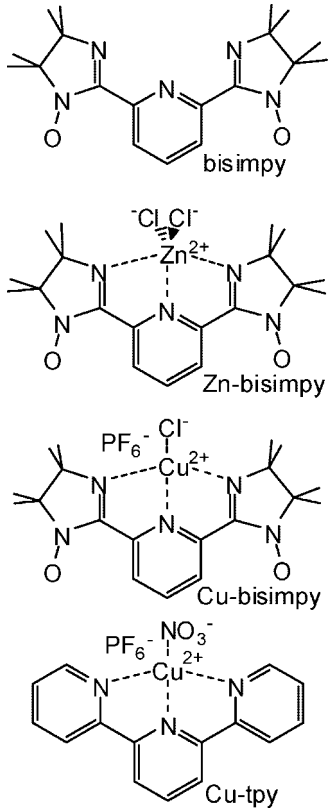

Figure 1. Molecular structures of biradical ligands (bisimpy), its zinc(II) and copper(II) complexes (Zn−bisimpy and Cu−bisimpy), and copper(II) complex with terpyridine (Cu−tpy). Solvent molecules which may coordinate along the axial directions are omitted for simplicity.

origin of the strong ferromagnetic coupling. In this paper, we have carried out multifrequency electron spin resonance (ESR) studies on the Cu−bisimpy complex and its related compounds.

Magnetic measurement using various highly sensitive magnetometers such as a superconducting quantum interference device, a Faraday magnetic balance and so on provides valuable information about bulk magnetism, but it is difficult to obtain the details of molecular interactions because of observation of the bulk magnetic moment. On the other hand, an ESR experiment allows us to separate the magnetic signals split by the fine interactions with the orbital angular moment, electron spin and nuclear spin. Hence, on the basis of the analysis of the ESR spectrum, we can clarify the structure of the magnetic orbitals. Furthermore, ESR experiments at different frequencies (in other words, multifrequency ESR spectroscopy) have several advantages compared with the conventional ESR technique, which uses a single X-band frequency of about 9.5 GHz.[21–25] Multifrequency ESR enables us to distinguish the field-dependent and -independent terms in the spin Hamiltonian dominating the spectral pattern. Because of this merit, the spectral analysis becomes easy, and magnetic parameters can be obtained with higher accuracy. Using multifrequency ESR spectroscopy, here we report a small Cu hyperfine coupling, a small g anisotropy and a large zero-field splitting for Cu−bisimpy, which arise from the covalent effect on the σ-type bonding between copper and nitrogens. The covalent bonding effect is probably a main reason for the strong ferromagnetic interaction, which would provide an important guidance for developing molecule-based magnets.

Experimental Section

The radical and biradical ligands were prepared by the reported method.[26] The metal complexes were synthesized by

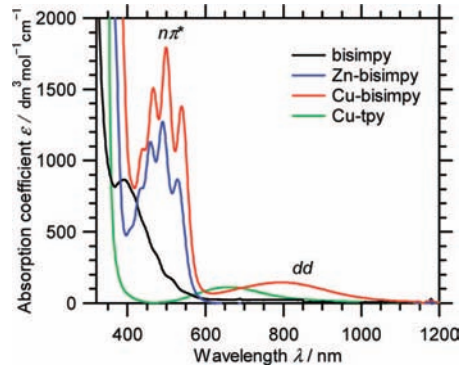

Figure 2. UV/vis/NIR-absorption spectra of bisimpy, Zn−bisimpy, Cu−bisimpy and Cu−tpy measured in CH_3CN at room temperature.

the method described in the previous paper.[19] The Cu^{2+} complex with terpyridine (Cu−tpy, Figure 1) was newly synthesized by stirring 2,2′;6′,2″-terpyridine (tpy, 0.94 mmol), $Cu(NO_3)_2$ (0.94 mmol) and Bu_4NPF_6 (1.80 mmol) in methanol (MeOH, 100 cm^3) with heating. $[Cu-tpy(NO_3)(MeOH)]PF_6$ produced in the MeOH solution was crystallized at 5 °C after heat filtration of the solution, offering blue rhombic crystals. X-ray analysis of the crystal clarified that the central Cu^{2+} ion has a square planar pyramidal coordination structure. Three nitrogens of the tpy ligand and one oxygen of the nitrate ion are coordinated in equatorial positions. In the single crystal, the MeOH oxygen sits at the axial position (see Supporting Information). Nitrile and alcohol solvents obtained from standard sources were used as a glassy matrix for low temperature measurements without further purification. For the ESR measurements, the samples were diluted in the organic solvents at a concentration of $10^{-3}-10^{-4}$ mol/dm^3 to prevent the intermolecular magnetic interaction and sealed in quartz tubes. Measurements were performed at S (3.0 GHz), X (9.5 GHz), Q (34.1 GHz) and W (94.0 GHz) band frequencies using several spectrometers (Bruker ESP300, ESP380E and ELEXES E600). The X-band spectrometer was equipped with a microwave cavity with a rectangular TE_{102} mode. Cylindrical cavities with a TE_{011} mode were used at other frequencies. Helium flow systems (Oxford ESR900 and CF935) were also used for the ESR measurements at low temperatures. Electronic spectra were recorded on a spectrophotometer (Jasco V-570).

Results

Figure 2 shows the optical absorption spectra of Cu−bisimpy and its related compounds. The bisimpy shows a broad absorption band in the range of 350−570 nm attributed to a well-known nπ* transition of the imino nitroxide radical, which is characterized by a low absorption coefficient (ε) of ∼500 dm^3mol^{-1} cm^{-1} and a vibronic structure at 1350−1500 cm^{-1} due to N−O or C═N stretching modes.[27–29] The ε of the nπ* band of bisimpy becomes almost double that of the imino nitroxide radical, consistent with the presence of two imino nitroxide radical sites in the molecule. The nπ* band of Zn−bisimpy has a more prominent progression, and a second vibronic line (the 1−0 line) becomes the most intense. According to the Franck−Condon principle, the change in the vibronic pattern is basically interpreted by the increase in planarity and rigidity of the molecular structure of bisimpy caused by complexation with Zn^{2+}. In the spectrum of Cu−bisimpy, not only the nπ* band with the prominent vibronic structure but also a weak and broad dd transition due to Cu^{2+} appeared in the long wavelength side. The position of the dd band gives a

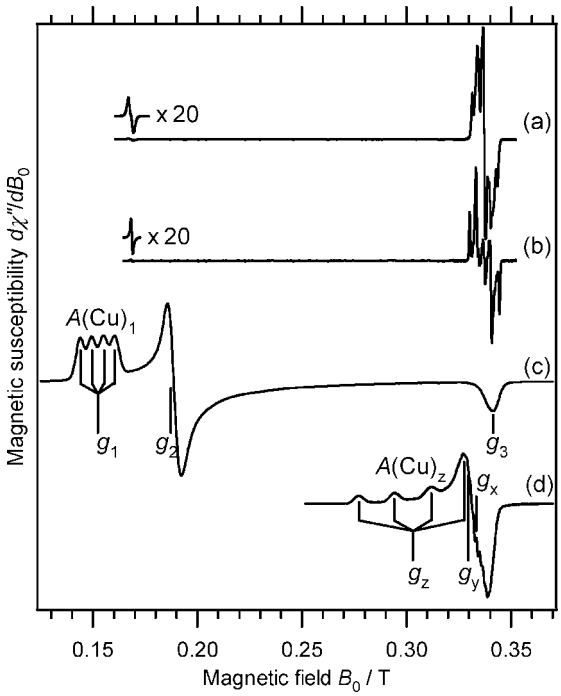

Figure 3. Randomly oriented ESR spectra of bisimpy (a), Zn−bisimpy (b), Cu−bisimpy (c) and Cu−tpy (d) in a rigid glassy matrix observed at X-band frequency.

ligand field splitting (Δ) of $\sim 1 \times 10^4$ cm^{-1}, which would correspond to a gap between the d_{xy} and $d_{x^2-y^2}$ orbitals of the central metal copper in the square planar coordination of bisimpy and Cl^- ion. The assignment of the dd band was confirmed by comparison with the spectrum of Cu−tpy, showing a weak, broad dd band at 500−900 nm ($\Delta \approx 1.2 \times 10^4$ cm^{-1}).

X-band ESR spectra for the series of compounds observed in frozen glassy matrices are shown in Figure 3. Bisimpy shows strong multiplet lines around 0.335 T and a weak signal at 0.167 T, which form a typical randomly oriented spectrum of a triplet state having $g = 2.005$ and zero-field parameters of $|D| = 168$ MHz and $|E| = 15$ MHz. Zn−bisimpy, a complex with a diamagnetic Zn^{2+} ion, also shows a similar triplet spectrum with $g = 2.005$, $|D| = 201$ MHz and $|E| = 9$ MHz. These spectra increased in intensity on lowering the temperature, indicating a triplet ground state. Within the point dipolar approximation,[30] the estimated $|D|$ values of the triplet states are reduced to the interspin distances of 0.78 and 0.73 nm for bisimpy and Zn−bisimpy, respectively. Because these distances are comparable to the separation between the molecular centers of the imino nitroxides, it can be said that the triplet ground states of these compounds are composed from the singly occupied molecular orbitals of two organic monoradicals.

On the other hand, Cu−bisimpy, a Cu^{2+} complex with a square coordination geometry, showed a remarkably different spectrum, which has an orthorhombic shape of a doublet state without a fine structure. The apparent principle g values of $g_1 = 4.41$, $g_2 = 3.56$ and $g_3 = 2.00$ were obtained from the three canonical resonance fields. Quartet hyperfine lines split by 5.47 mT (153 MHz) due to Cu nucleus spin ($I = 3/2$) also appear at the lowest canonical field corresponding to g_1. No temperature dependence of the spectral shape was observed from 3.5 to 150 K. In the case of Cu−tpy in a doublet state that has a structure similar to that of Cu−bisimpy, a nearly orthorhombic spectrum of $g_z = 2.256$, $g_y = 2.074$ and $g_x = 2.050$ was observed, which is different from those for Cu−bisimpy. Even compared with a wide variety of doublet state Cu(II) complexes in square planar coordination ($g_{\|} = 2.045-2.074$, $g_{\perp} = 2.165-2.349$),[31] the apparent **g** tensor elements of Cu−bisimpy are substantially large. Furthermore, the spectrum of Cu−bisimpy is completely distinguished from those for Cu(II) radical complexes[32–34] and double spin-labeled Cu(II) complexes chelated by carboxylic acid groups,[33,34] which have no large magnetic interactions. The characteristics of Cu−bisimpy are considered to being a Kramers' doublet state originated from a quartet state with large splittings among the spin sublevels even at zero field. When the $|D|$ value exceeds the microwave energy ($h\nu_{MW}$), some of the ESR allowed transitions cannot be detected at any strength and angle of the magnetic field. As a result of the loss of some transitions, the relation between the apparent and true g values can be approximately written as[35–37]

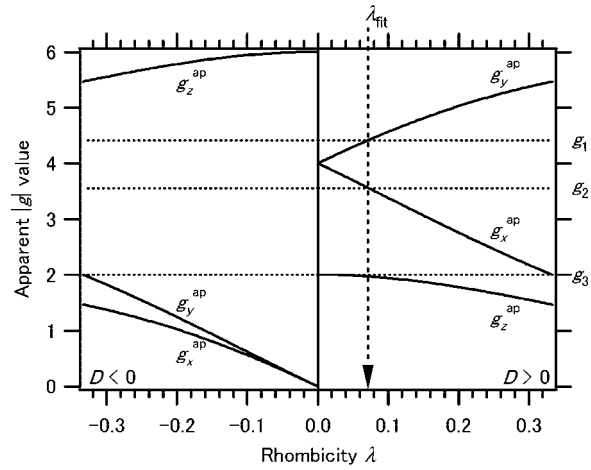

Figure 4. Diagram of apparent g values (g^{ap}) of Kramers' doublet against rhombicity (λ) of the zero-field splitting of the state with $S = 3/2$. The dotted lines are the g values of Cu−bisimpy obtained from the S- and X-band ESR spectra.

$$\begin{cases} g_x^{ap} = g_x\left[1 \pm \dfrac{(1-3\lambda)}{M}\right] \\ g_y^{ap} = g_y\left[1 \pm \dfrac{(1-3\lambda)}{M}\right] \\ g_z^{ap} = g_z\left[1 \mp \dfrac{2}{M}\right] \end{cases} \quad (1)$$

because

$$\lambda = \frac{E}{D}, \quad M = \sqrt{1+3\lambda^2} \quad (2)$$

The upper signs refer to the case of $D > 0$ in which the sublevels of $m_S = \pm 1/2$ are the ground levels and the lower signs in the case of $D < 0$ of the $m_S = \pm 3/2$ ground levels. If we assume that all of the true g factors are equivalent to g_e ($g_x = g_y = g_z \approx g_e = 2.00$), the observed apparent g factors were reproduced well when employing a positive D and $\lambda = 0.073$ as illustrated in Figure 4.

In order to the examine validity of the Kramers' doublet of Cu−bisimpy, we measured the ESR spectra using several microwaves with different frequencies. As shown in Figure 5, the spectrum of Cu−bisimpy drastically depended on the frequency. The spectrum measured at 3.0 GHz has a Kramers' doublet shape with $g_1 = 4.49$, $g_2 = 3.60$ and $g_3 = 2.00$, which are nearly the same as the 9.5 GHz-spectrum. At the g_1 canonical field, the quartet lines caused by the Cu-hyperfine interaction with $A(Cu)_1 = 5.47$ mT (153 MHz) become clearer than that of the 9.5 GHz-spectrum, indicative of the sharpening of the resonance line due to the decrease in the magnetic fields.

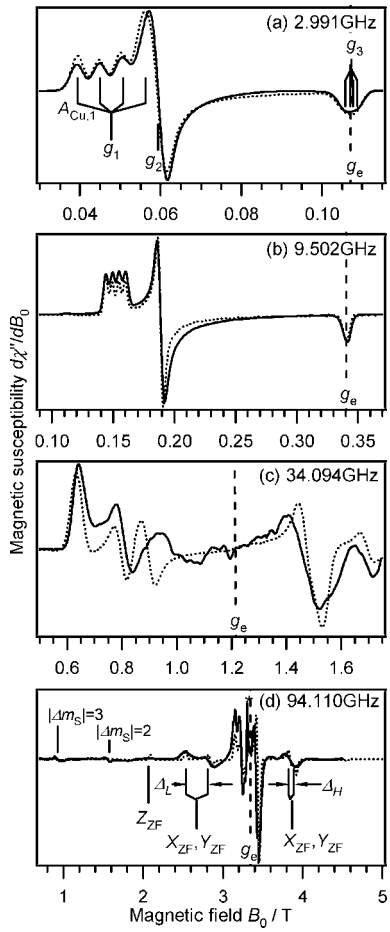

Figure 5. Multifrequency ESR spectra of Cu−bisimpy (solid line) in *n*-butyronitrile rigid glassy matrix and their simulations (broken line). Asterisk in d denotes double quantum transitions.

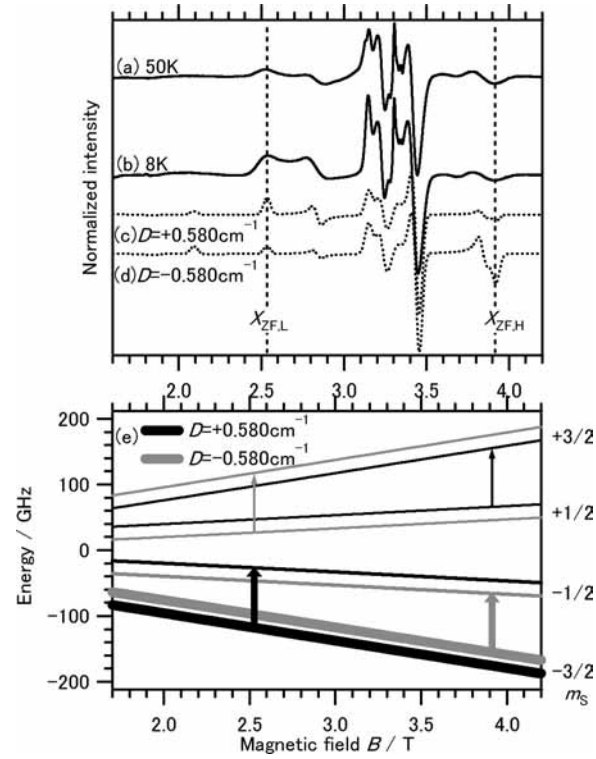

Figure 6. Temperature dependence of the 94 GHz-spectrum of Cu−bisimpy observed in *n*-butyronitrile rigid glassy matrix (a and b). The broken lines are spectra calculated with the spin population at 8 K assuming $D = +17.4$ GHz (c) and -17.4 GHz (d). (e) Magnetic field dependence of the quartet spin sublevels in the case of $B \,//\, X_{ZF}$. The line width of the sublevels reflects the population at very low temperatures, and the arrows indicate resonances between the $\pm 1/2$ and $\pm 3/2$ sublevels.

Because of this line-sharpening, the signal at the g_3 canonical field changes to a trapezoidal shape, suggesting the presence of other quartet lines split by a small Cu-hyperfine. When a microwave of 34 GHz was employed, many peaks appeared in the region from 0.58 to 1.8 T. The signals at higher than 1.217 T corresponding to a g smaller than g_e cannot be understood only by the resonances within the Kramers' doublet. At 34 GHz, a broad signal was also detected near 0 T, suggesting a $2|D|$ value comparable to the microwave energy. Inhomogeneous line-broadening due to large zero-field interaction and/or strain effects results in disappearance of the Cu-hyperfine structures in the 34 GHz-spectra. Measurement at 94 GHz allowed us to record a nearly symmetric spectrum having fine structures centered at 3.33 T (B_{SC}). However, there are no quartet lines of Cu-hyperfine interaction. Compared with a typical powder pattern of the quartet state,[38,39] the strong peaks at 3.1−3.5 T stem from the allowed transitions between the spin sublevels with $m_S = \pm 1/2$. The weak signals out of the central field region are assigned to the allowed transitions of $m_S = 3/2 \leftarrow m_S = 1/2$ and $m_S = -1/2 \leftarrow m_S = -3/2$. The other weak satellite peaks in the low field region are considered to be the forbidden transitions of $|\Delta m_S| = 2$ and 3 on the basis of their field positions of $B_{SC}/2$ and $B_{SC}/3$. We could roughly estimate the $|D|$ value of 16.5−18.0 GHz from the field position of the outermost allowed signals, which are attributed to the transitions at the resonance field along the maximum splitting axis of zero-field interaction (Z_{ZF}) and would appear at the positions separated by $2|D|$ from B_{SC}. The middle allowed canonical signals at the low field of 2.7 T, which are the transition at the resonance fields parallel to the other principle axes (X_{ZF}, Y_{ZF}), are split into two lines separated by Δ_L, while the high field ones at 3.85 T remain almost at one line ($\Delta_H \approx 0$). The obvious splitting of the middle canonical signals indicates a nonzero E value of the zero-field interaction. This is consistent with the fact of $\lambda \neq 0$ concluded from the analysis of the orthorhombic spectrum at 9.4 GHz. The nonequivalent separation of $\Delta_L \neq \Delta_H$ clearly results from anisotropic g-factor along the X_{ZF} or Y_{ZF} axis.

In order to determine the sign of the D value of Cu−bisimpy, the temperature dependence of the 94 GHz spectrum in which the fine structure is well-resolved. As shown in Figure 6, the middle canonical signals at the low field side indicated by $X_{ZF,L}$ increased in intensity in comparison with the high field one of $X_{ZF,H}$. At low temperature under a strong magnetic field, a large population in the lowest sublevel is achieved so that the resonance with the microwave connected to the lowest sublevel becomes more pronounced than others. In the case of $B//X_{ZF}$, the resonances with the lowest sublevel take place in the low field side, if D is positive. When D is negative, the resonances concerned occur in the high field. Based on this consideration, the relative intensity growth of the low field signals at low temperature proves that the D value of Cu−bisimpy is positive, consistent with the conclusion from the analysis of the Kramers' doublet spectrum mentioned above.

To estimate the accurate magnetic parameters of Cu−bisimpy, we have performed spectral simulation for a powder pattern using an effective spin Hamiltonian consisting of three terms of Zeeman ($\mathbf{H}_{ZI}$), zero-field ($\mathbf{H}_{ZF}$) and Cu-hyperfine ($\mathbf{H}_{HF}$) interactions.

$$\mathbf{H}_S = \mathbf{H}_{ZI} + \mathbf{H}_{ZF} + \mathbf{H}_{HF} = \mu_B \mathbf{B} \cdot \mathbf{g} \cdot \mathbf{S} - \mu_n \mathbf{B} \cdot \mathbf{g}_{Cu} \cdot \mathbf{I}_{Cu} + \mathbf{S} \cdot \mathbf{D} \cdot \mathbf{S} + \mathbf{S} \cdot \mathbf{A}(Cu) \cdot \mathbf{I}_{Cu}. \quad (3)$$

B is the external magnetic field vector. μ_B and μ_n are Bohr and nuclear magnetons. **g** and $\mathbf{g}_{Cu}$ are **g** tensors of the electron and the Cu nucleus. **S** and $\mathbf{I}_{Cu}$ denote spin operators for the electron ($S = 3/2$) and the Cu nucleus ($I = 3/2$). **D** and **A**(Cu) stand for tensors of zero-field and hyperfine interactions. The eigenvalues (E_n) and eigenvectors (Φ_n) were obtained from a numerical matrix diagonalization of $\mathbf{H}_S$, in which simple product functions between the electron and nuclear spin parts ($|\phi_S\phi_I\rangle$) were employed for a basis set (see Supporting Information). Spectrum depends on the locations of resonance field (B_r) given via the Bohr frequency relation of

$$E_f(\mathbf{B}_r) - E_i(\mathbf{B}_r) = h\nu_{MW} \quad (4)$$

and the squared magnitudes of the magnetic transition dipole moment of

$$w_{ij} = |\langle \Phi_j | \mathbf{B}_1 \cdot \mathbf{g} \cdot \mathbf{S} | \Phi_i \rangle|^2 \quad (5)$$

where i and f are indices for the initial and final spin sublevels, respectively, and B_1 is a vector of the magnetic field component of the microwave.[40,41] Hence, we first determined the resonance fields from the eigenvalues and the transition probabilities (w) from the eigenvectors, according to the equations above. The resonance lines with a certain individual line width calculated at each angle were then integrated over a proper range of the orientations of B_1 as well as B to create a powder pattern spectrum (S).

$$S(B, \nu_{MW}, \theta, \phi, \chi) \propto \int_0^{\infty} \int_0^{2\pi} \int_0^{\pi} \int_0^{2\pi} \sum_{f=i+1}^{m_S} \sum_{i=-m_S}^{m_S} w_{ij} p(T) f(|\mathrm{B} - \mathrm{B}_0|, \Gamma)\, d\chi \sin\theta\, d\theta\, d\phi\, dB_0. \quad (6)$$

Here p is the population difference which is a function of temperature (T) and f is a resonance line shape function for which the Gaussian with a half-width-of-half-maximum (Γ) has been taken in this paper. θ and ϕ are the colatitude and azimuth of **B** in a molecular axis system. χ is an angle variable to specify the direction of $\mathbf{B}_1$ in the plane perpendicular to **B**. The simulated spectra are depicted by broken lines in Figure 5, and the optimized ESR parameters are listed in Table 1. The **g** and **D** tensor elements were mainly determined by fitting the spectra of the high frequencies of 34 and 94 GHz, while the **A**(Cu) tensor elements were obtained from the low-frequency spectral simulations. Gaussian resonance lines with Γ values of 39, 84, 700 and 841 MHz were adopted for 3.0, 9.5, 34 and 94 GHz-spectral simulations, respectively. The Γ value does not increase smoothly with the increase in frequency, but it suddenly changes by almost 10-fold when the spectrum changes from a Kramers' doublet pattern to a normal quartet pattern. Such nonlinear frequency dependence of resonance line width is interpreted in terms of a distribution of zero-field splittings rather than g-strain. The fine agreement between the observed and simulated spectra at 34 GHz could not be obtained by any parameter set in the calculation based on summation of the static spectra. Maybe this unsolved disagreement comes from the neglect of a dynamic effect in the simulation, such as spin relaxations around 0.9 T where many turnovers and crosses of spin sublevels take place because of the anisotropic zero-field interaction of Cu−bisimpy. Another thing impossible to simulate is that the sharp line at B_{SC} of the 94 GHz spectrum was not reproduced at all. The observed sharp line would be a double-quantum line that increases in intensity with an increase in the resonance field.[42,43] The simulation spectra in Figure 6 show how the sign of the D value affects the relative intensity of well-resolved peaks in the high field spectrum detected at low temperatures. The simulation using a positive D value reproduces the observed one.

Discussion

In this paper, the multifrequency ESR experiments clarified the magnetic parameters of Cu−bisimpy as summarized in Table 1. High-frequency experiments elucidated that the **g** tensor elements for Cu−bisimpy were almost uniaxial like many square planar Cu(II) complexes with $g_{\parallel} > g_{\perp} \approx g_e$. The hyperfine coupling constants of Cu(II) determined by low-frequency measurements were the orthorhombic of $A(Cu)_z > A(Cu)_x > A(Cu)_y$. The drastic frequency dependence of the spectrum also elucidated that Cu−bisimpy possesses an extremely large positive D value. These magnetic parameters for the ground quartet state that is a magnetic isosceles triangle cluster among one doublet Cu^{2+} and two doublet imino nitroxide radicals (impy) under the strong exchange limit ($|J| \gg |D|$) can be written by[44]

$$\mathbf{g} = \frac{1}{3}(\mathbf{g}_{Cu} + 2\mathbf{g}_{impy}), \quad (7)$$

$$\mathbf{A}(Cu) = \frac{1}{3}(\mathbf{A}(Cu)_{Cu} + 2\mathbf{A}(Cu)_{impy}) \approx \frac{1}{3}\mathbf{A}(Cu)_{Cu}, \quad (8)$$

$$\mathbf{D} = \frac{1}{6}(\mathbf{D}_{impy,impy} + 2\mathbf{D}_{Cu,impy}) \approx \frac{1}{3}\mathbf{D}_{Cu,impy}. \quad (9)$$

$\mathbf{g}_i$ and $\mathbf{A}_i$ are the **g** and hyperfine tensors for the ith spins. $\mathbf{D}_{i,k}$ is the fine structure tensor between the i and k spins. The unpaired electron of impy is in a π^* orbital that is orthogonal to the five-member ring plane containing the N−O group and obviously delocalized on the molecular framework. [45,46] In bisimpy, its solution ESR spectrum at room temperature exhibited isotropic hyperfine couplings due to five nitrogen atoms in two imino nitroxide groups and a pyridine linker (see Supporting Information). These splittings are consistent with full delocalization of the unpaired electron on a π conjugated

TABLE 1: Magnetic properties obtained from the ESR experiments of Cu−bisimpy and its related complexes

								Cu	N[b]			
complex	J/cm^{-1}[a]	g_x	g_y	g_z	$\|D\|$ /GHz	$\|E\|$ /GHz	$\|\lambda\|$	$\|A_x\|$ /MHz	$\|A_y\|$ /MHz	$\|A_z\|$ /MHz	$\|A_{iso}\|$ /MHz	
bisimpy	+6.5	2.005	2.005	2.005	0.168	0.015	0.089	−	−	−	12.2 (2)[c] 6.4 (2)[c] 0.2 (1)[c]	
Zn−bisimpy	+6.5	2.006	2.006	2.006	0.201	0.009	0.045	−	−	−		
Cu−bisimpy	+165	2.02	2.01	2.08	+17.4[d]	−1.0[d]	0.059	42.0	<14	153		
Cu−tpy	–	2.050	2.074	2.256	−	−	−	42	42	476	40.6 (3)[c]	

[a] Taken from ref 19. [b] Nitrogen nuclei in ligand. [c] Number of equivalent atoms. [d] Sign is also determined experimentally.

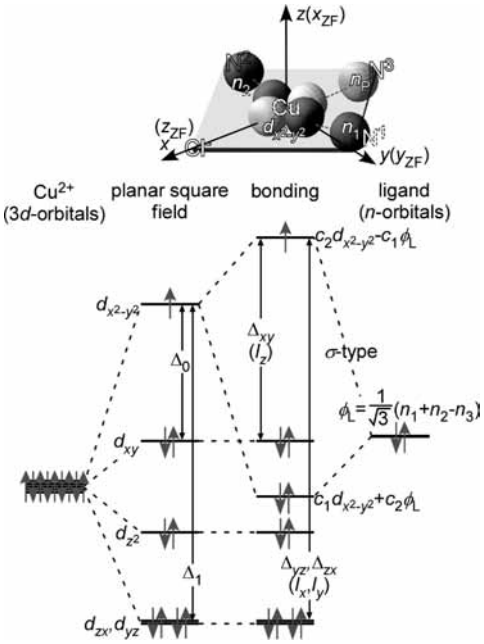

Figure 7. Geometry and energy level of symmetry-adopted molecular orbitals forming a σ type of Cu-ligand bond with the singly occupied orbital ($3d_{x^2-y^2}$) of Cu(II) in Cu−bisimpy with a square planar structure. *xyz* indicates the principle axes for $3d_{x^2-y^2}$, **g**, and **A**(Cu) tensors. xyz_{ZF} is for the zero-field interaction.

system. The density functional theory also indicates a substantial spin density on the nitrogens which connect with the central metal copper.[19] The semioccupied orbital (SOMO) of Cu(II) in square planar coordination is basically the $3d_{x^2-y^2}$ orbital as shown in Figure 7.

The $\mathbf{g}_{impy}$ can be approximated to be an isotropic value of 2.005−2.006 from the literature values[47] and the observed $\mathbf{g}_{bisimpy}$ (see Table 1). The inverse operation of the observed anisotropic **g** tensor according to eq (7) results in the fact that the $\mathbf{g}_{Cu}$ tensor has the elements of $(g_{Cu,x}, g_{Cu,y}, g_{Cu,z}) = (2.04, 2.01, 2.22)$. It is noteworthy that the estimated **g** tensor elements are small, compared with the theoretical $g_{Cu,z}$ value (∼2.6) that is calculated using the unit spin density on Cu, Δ_0 of 1×10^4 cm^{-1} estimated from the observed dd absorption of Cu−bisimpy and λ_{Cu} of 829 cm^{-1} determined spectroscopically.[41,48] Because the covalent bonding effect tends to occur in Cu complexes coordinated with nitrogens,[49] it is reasonable that the small $\mathbf{g}_{Cu}$ anisotropy in Cu−bisimpy is discussed on the basis of the delocalization of Cu spin due to the covalent bonding effect. In order to estimate the σ bonding character between the $d_{x^2-y^2}$ and the ligand orbital (ϕ_L) in a square plane, therefore, we use a symmetry-adapted combination of nonbonding orbitals (*n*) belonging to three nitrogen atoms in the bisimpy ligand as shown in Figure 7.Two σ bonds (Ψ_b and Ψ_a) are described by the bonding and antibonding combination between the $d_{x^2-y^2}$ and ϕ_L orbitals using the normalization coefficients of *c*.

$$\begin{cases} \psi_b = c_1 d_{x^2-y^2} + c_2 \varphi_L \\ \psi_a = c_2 d_{x^2-y^2} - c_1 \varphi_L \end{cases} \quad \text{because} \quad |c_1|^2 + |c_2|^2 = 1 \qquad (10)$$

The antibonding orbital of Ψ_a becomes SOMO in the complex. Assumed that only the angular momentum about the Cu ion is significant, in the case of square planar Cu(II) complexes, the deviations of *g* values from g_e are expressed by the following.[50,51]

$$\Delta g_z = g_z - g_e = \frac{8\lambda_{Cu}}{\Delta_{xy}}|c_2|^2. \qquad (11)$$

Here, we assumed that the principal axis having the largest *g* value is the out-of-plane axis of *z*. To reproduce the experimentally determined Δg_z of 0.22 using eq (11), $|c_2|^2$; must range from 0.4 to 0.5, indicating a heavy covalent bonding effect.

The hyperfine coupling constant of Cu (**A**(Cu)) is also indicative of modification of the $d_{x^2-y^2}$ SOMO in a square plane. As expressed in eq 8, only the $\mathbf{A}(Cu)_{Cu}$ term becomes significant on the assumption that the hyperfine coupling of the Cu nucleus with the electrons in ligand orbitals is negligible. The $\mathbf{A}(Cu)_{Cu}$ can be written by

$$A(Cu)_{Cu,z} = -\frac{\mu_0}{4\pi}\gamma_e\gamma_{Cu}\langle r^{-3}\rangle\left(\frac{4}{7} + \Delta g_{||} + \frac{3}{7}\Delta g_{\perp}\right) \approx -\frac{4}{7}P_d, \qquad (12)$$

$$A(Cu)_{Cu,x,y} = \frac{\mu_0}{4\pi}\gamma_e\gamma_{Cu}\langle r^{-3}\rangle\left(\frac{2}{7} - \frac{11}{14}\Delta g_{\perp}\right) \approx \frac{2}{7}P_d. \qquad (13)$$

in the first approximation.[52] Here μ_0, γ and λ_{Cu} are the permeability of a vacuum, the magnetogyric ratio and the spin−orbit coupling constant of Cu, respectively. The observed Δg in order of 10^{-2} is small enough compared with the first terms for the spin population part of 10^{-1} order. Hence, the anisotropic hyperfine coupling of Cu is regarded to be proportional to the spin population in the $3d_{x^2-y^2}$ orbital. Using eq 8, the anisotropic elements of $A(Cu)_{Cu,z} = (1.0 \pm 0.2) \times 10^8$ Hz and $A(Cu)_{Cu,x} \approx A(Cu)_{Cu,y} = -(5.3 \pm 0.8) \times 10^7$ Hz were estimated from the observed A(Cu). These values are reduced to the spin density of 0.13−0.18 on the central Cu atom (ρ_{Cu}), from the comparison with the theoretical weighted mean value of the 3d orbitals for two stable isotopes of^{63} Cu (69.2%) and^{65} Cu (30.8%).[53] The ρ_{Cu} value of almost half of 1/3 indicates a reduction in spin density in the $3d_{x^2-y^2}$ of Cu, reflecting a covalent bonding effect with the ligand. The small spin density on Cu is quantitatively consistent with the mixing ratio determined by the *g* anisotropy.

Cu−bisimpy possesses a large positive *D* value of +17.4 GHz, which is hardly explained in terms of the triplet biradical ligand that has a small dipolar interaction of $|D| = 0.168$ GHz. Like eq (9), therefore, the total **D** tensor is approximated as the interaction term ($\mathbf{D}_{Cu,impy}$) between the unpaired electrons in the metal and ligand. If the spin−orbit coupling with excited states due to the central metal is substantially large, the anisotropy of **D** and **g** tensors become large and the sign of *D* value should be negative.[54,55] However this is not the case for the unusual large zero-field splitting in Cu−bisimpy. *D* for the Cu−bisimpy complex is positive, and the principal axis system for the zero-field interaction (xyz_{ZF}) is not in accord with that of the **g** tensor, as illustrated in Figure 7. The clear Cu hyperfine splitting in one of the two perpendicular transitions at the low-frequency spectra indicates that the most anisotropic axis (z_{ZF}) was perpendicular to the *z* axis and was oriented to the *x* axis. In consequence, the σ bonding between the metal and ligand probably is the primary origin of the large *D* value. The covalent bond reduces the spin density on Cu but increases that on the nonbonding orbitals of nitrogens. Because imino nitroxide radicals generally have large π spin densities on N^1 and N^2, the dipolar interactions between unpaired electrons individually occupying the orthogonal orbitals on the same nitrogens become effective. The nπ interaction that is the same as carbene is large[56,57] because of its nature of one-centered integrals for the

dipolar and spin−orbit interactions.[58–65] The $n\pi$ interaction due to the carbene configuration should have the maximum splitting axis perpendicular to both the n- and π-orbitals, which is almost parallel to the Cu−Cl coordination direction. The z_{ZF} axis is within the molecular plane, although its exact direction is unknown, and agrees with the combination direction of the maximum splitting axes for the one-centered interactions on N^1 and N^2 being within the molecular plane. The in-plane z_{ZF} axis supports the carbene configuration for the large D value.

The magnetic properties obtained in the ESR experiments on the Cu−bisimpy complex clarified the covalent bonding effect between Cu and the radical ligand that leads to the carbene configuration on the nitrogens. It is reported that, on the other hand, a nitroxyl radical complex of Cu having $|D| = 5.13$ GHz shows a weak ferromagnetic interaction ($J = 13$ cm^{-1}).[8] In the case of the Cu-radical complex, a correction associated with the covalent bonding effect inducing one-centered magnetic interactions is suggested. The strong ferromagnetic interaction of Cu−bisimpy can also be interpreted in terms of the carbene configuration. The overlap between the magnetic orbitals on the same atom is much larger than that among multicentered orbitals. The n- and π-orbitals on the nitrogens of bisimpy are orthogonal to each other, which is a necessary condition for strong ferromagnetic interaction. These two factors originating from the covalent bonding effect would induce a large positive J value.

Conclusions

Based on the ESR experiments on Cu−bisimpy and its related compounds, we found peculiarity in the magnetic orbitals of Cu−bisimpy caused by the σ-type covalent bonding effect. Multifrequency ESR spectroscopy clarified a reliable set of magnetic parameters of Cu−bisimpy, which had a small g anisotropy and small hyperfine coupling with Cu but huge zero-field splitting. The characteristics of the magnetic parameters indicate that the covalent bonding causes the carbene-like electronic configuration on the nitrogens in the two imino nitroxide radicals, which is the main reason for the strong ferromagnetic coupling.

Acknowledgment. T.I. thanks Prof. K. Akiyama (Tohoku University) for his valuable discussion and Prof. S. Yamauchi (Tohoku University) for his providing the opportunity for the W-band ESR measurements. Spectral simulations were performed using the supercomputing resources of the Information Synergy Center, Tohoku University. This research was financially supported by PRESTO from the JST.

Supporting Information Available: This material is available free of charge via the Internet at http://pubs.acs.org.

References and Notes

(1) Kahn, O. *Molecular Magnetism*; VCH: New York, 1993.
(2) *Molecular Magnetism: New Magnetic Materials*; Itoh, K.; Kinosita, M. Eds.; Wiley: Tokyo, 2000.
(3) Gatteschi, D.; Sessoli, R.; Villain, J. *Molecular Nanomagnets*; Oxford Univ. Press: Oxford, 2006.
(4) Jain, R.; Kabir, K.; Gilroy, J. B.; Mitchell, K. A. R.; Wong, K.; Hicks, R. G. *Nature* **2007**, *445*, 291.
(5) Caneshi, A; Gatteschi, D.; Rey, P. *Prog. Inorg. Chem.* **1991**, *39*, 331.
(6) Ovcharenko, V. I.; Maryunina, K. Y.; Fokin, S. V.; Tretyakov, E. V.; Romanenko, G. V.; Ikorskii, V. N. *Russ. Chem. Bull. Int. Ed.* **2004**, *53*, 2406–2427.
(7) Caneshi, A.; Gatteschi, D.; Sessoli, R.; Rey, P. *Acc. Chem. Res.* **1989**, *22*, 392.
(8) Bencini, A.; Benelli, C.; Gatteschi, D.; Zanchini, C. *J. Am. Chem. Soc.* **1984**, *106*, 5813.
(9) Caneshi, A.; Gatteschi, D.; Laugier, J.; Rey, P. *J. Am. Chem. Soc.* **1987**, *109*, 2191.
(10) Caneshi, A.; Gatteschi, D.; Grand, A.; Laugier, J.; Pardi, L.; Rey, P. *Inorg. Chem.* **1988**, *27*, 1031.
(11) Cabello, C. I.; Caneshi, A.; Carlin, R. L.; Gatteschi, D.; Rey, P.; Sessoli, R. *Inorg. Chem.* **1990**, *29*, 2582.
(12) Musin, R. N.; Schastnev, P. V.; Malinovskaya, S. A. *Inorg. Chem.* **1992**, *31*, 4118.
(13) Fedin, M. V.; Veber, S. L.; Gromov, I. A.; Ovcharenko, V. I.; Sagdeev, R. Z.; Schweiger, A.; Bagryanskaya, E. G. *J. Phys. Chem. A.* **2006**, *110*, 2315.
(14) Luneau, D.; Rey, P.; Laugier, J.; Fries, P.; Caneschi, A.; Gatteschi, D.; Sessoli, R. *J. Am. Chem. Soc.* **1991**, *113*, 1245.
(15) Cogne, A.; Laugier, J.; Luneau, D.; Rey, P. *Inorg. Chem.* **2000**, *39*, 5510.
(16) Tanaka, K.; Kozaki, M.; Shiomi, D.; Sato, K.; Takui, T.; Okada, K. *Polyhedron* **2003**, *22*, 1803.
(17) Tretyakov, E. V.; Eltsov, I. V.; Fokin, S. V.; Shvedenkov, Y. G.; Romanenko, G. V.; Ovcharenko, V. I. *Polyhedron* **2003**, *22*, 2499.
(18) Stevens, J. E.; Brook, D. J. R.; Abeyta, V. W. *Polyhedron* **2003**, *22*, 2241.
(19) Oshio, H.; Yamamoto, M.; Ito, T.; Kawauchi, H.; Koga, N.; Ikoma, T.; Tero-Kubota, S. *Inorg. Chem.* **2001**, *40*, 5518.
(20) Takano, Y.; Kitagawa, Y.; Onishi, T.; Yoshioka, Y.; Yamaguchi, K.; Koga, N.; Iwamura, H. *J. Am. Chem. Soc.* **2002**, *124*, 450.
(21) Ikoma, T.; Akiyama, K.; Tero-Kubota, S. *Mol. Phys.* **1999**, *96*, 813.
(22) Ikoma, T.; Zhang, Q.; Saito, F.; Akiyama, K.; Tero-Kubota, S.; Kato, T. *Bull. Chem. Soc. Jpn.* **2001**, *74*, 2303.
(23) Ikoma, T.; Okada, S.; Nakanishi, H.; Akiyama, K.; Tero-Kubota, S.; Möbius, K.; Weber, S. *Phys. Rev. B* **2002**, *66*, 014423.
(24) Ikoma, T.; Akiyama, K.; Tero-Kubota, S. *Phys. Rev. B* **2005**, *71*, 195206.
(25) Grinberg, O., Berliner, L. J., Eds. *Very High Frequency (VHF) ESR/EPR*; Biological Magnetic Resonance, Vol. 22; Kluwer Academic/Plenum Publishers: New York, 2004.
(26) Ulrich, G.; Ziessel, R. *Tetrahedron Lett.* **1994**, *35*, 1215.
(27) Ullman, E. F.; Osiecki, J. H.; Boocock, D. G. B.; Darcy, R. *J. Am. Chem. Soc.* **1972**, *94*, 7049.
(28) Zoppellaro, G.; Ivanova, A.; Enkelmann, V.; Geies, A.; Baumgarten, M. *Polyhedron* **2003**, *22*, 2099.
(29) Zoppellaro, G.; Geies, A.; Enkelmann, V.; Baumgarten, M. *Eur. J. Org. Chem.* **2004**, 2367.
(30) $D = -1.5(g\mu_B)^2/r^3$. Carrington, A.; McLachlan, A. D. *Introduction to Magnetic Resonance*; Harper & Row: London, 1967; p 117.
(31) Kivelson, D.; Neiman, R. *J. Chem. Phys.* **1961**, *35*, 149.
(32) Zagdeev, R. Z.; Molin, Y. N.; Sadikov, R. A.; Volodarsky, L. B.; Kurikova, G. A. *J. Magn. Reson.* **1973**, *9*, 13.
(33) Dalal, D. P.; Eaton, S. S.; Eaton, G. R. *J. Magn. Reson.* **1981**, *42*, 277.
(34) Eaton, S. S.; More, K. M.; Sawant, B. M.; Eaton, G. R. *J. Am. Chem. Soc.* **1983**, *105*, 6560.
(35) Pilbrow, J. R. *J. Magn. Reson.* **1978**, *31*, 479.
(36) Drulis, H.; Dyrek, K.; Hoffmann, K. P.; Hoffmann, S. K.; Weselucha-Birczyńska, A. *Inorg. Chem.* **1985**, *24*, 4009.
(37) Fukui, K.; Ohya-Nishiguchi, H.; Hirota, N. *Bull. Chem. Soc. Jpn.* **1991**, *64*, 1205.
(38) Brickmann, J.; Kothe, G. *J. Chem. Phys.* **1973**, *59*, 2807.
(39) Weissman, S. I.; Kothe, G. *J. Am. Chem. Soc.* **1975**, *97*, 2537.
(40) Pilbrow, J. R. *Transition Ion Electron Paramagnetic Resonance*; Clarendon: Oxford, 1990.
(41) Atherton, N. M. *Principles of Electron Spin Resonance*; Ellis Horwood and Prentice Hall: New York, 1993, p 211.
(42) van Dam, P. J; Klaassen, A. A. K.; Reijerse, E. J.; Hagen, W. R. *J. Magn. Reson.* **1998**, *130*, 140.
(43) Collison, D.; Helliwell, M.; Jones, V. M.; Mabbs, F. E.; McInnes, E. J. L.; Riedi, P. C.; Smith, G. M.; Pritchard, R. G.; Cross, W. I. *J. Chem. Soc., Faraday Trans.* **1998**, *94*, 3019.
(44) Bencini, A.; Gatteschi, D. *Electron Paramagnetic Resonance of Exchange Coupled Systems*; Springer-Verlag: Berlin, 1990.
(45) Ullman, E. F.; Call, L.; Osiechi, J. H. *J. Org. Chem.* **1970**, *35*, 3623.
(46) Barone, V.; Grand, A.; Luneau, D.; Rey, P.; Minichino, C.; Subra, R. *New. J. Chem.* **1993**, *17*, 545.
(47) Teki, Y.; Miyamato, S.; Nakatsuji, M.; Miura, Y. *J. Am. Chem. Soc.* **2001**, *123*, 294.
(48) Goodman, B. A.; Raynor, J. B. *J. Inorg. Nucl. Chem.* **1970**, *32*, 3406.
(49) (a) Maki, A. H.; McGarvey, B. R. *J. Chem. Phys.* **1958**, *29*, 31. (b) Maki, A. H.; McGarvey, B. R. *J. Chem. Phys.* **1958**, *29*, 35.
(50) Abragam, A.; Bleaney B. *Electron Paramagnetic Resonance of Transition Ions*; Oxford University Press: London, 1970; p 455, Chapter 7.16.
(51) Adam, C. D.; Owen, J.; Ziaei, M. E. *J. Phys. C: Solid State Phys.* **1978**, *11*, L117.
(52) Atherton, N. M. *Principles of Electron Spin Resonance*; Ellis Horwood and Prentice Hall: New York, 1993; p 206.

(53) Morton, J. R.; Preston, K. F. *J. Magn. Reson.* **1978**, *30*, 577.
(54) Blumberg, W. E.; Eisinger, J.; Geschwind, S. *Phys. Rev.* **1963**, *130*, 900.
(55) Marshall, S. A.; Kikuchi, T. T.; Reinberg, A. R. *Phys. Rev.* **1962**, *125*, 453.
(56) Wasserman, E.; Yager, W. A.; Kuck, V. J. *Chem. Phys. Lett.* **1970**, *7*, 409.
(57) Wasserman, E.; Kuck, V. J.; Hutton, R. S.; Yager, W. A. *J. Am. Chem. Soc.* **1970**, *92*, 7491.
(58) Higuchi, J. *J. Chem. Phys.* **1963**, *38*, 1237.
(59) Higuchi, J. *J. Chem. Phys.* **1963**, *39*, 1847.
(60) Palmiere, P.; Sink, M. L. *J. Chem. Phys.* **1976**, *65*, 3641.
(61) Langhoff, S. R.; Davidson, E. R. *Int. J. Quantum Chem.* **1973**, 759.
(62) Langhoff, S. R. *J. Chem. Phys.* **1974**, *61*, 3881.
(63) Langhoff, S. R. *J. Chem. Phys.* **1965**, *42*, 1549.
(64) McIver, J. W., Jr.; Hameka, H. F. *J. Chem. Phys.* **1966**, *45*, 767.
(65) Lounsbury, J. B. *J. Chem. Phys.* **1967**, *46*, 2193.

JP802810S